We are IntechOpen, the world's leading publisher of Open Access books Built by scientists, for scientists

4,800
Open access books available

122,000
International authors and editors

135M
Downloads

Our authors are among the

154
Countries delivered to

TOP 1%
most cited scientists

12.2%
Contributors from top 500 universities

CLARIVATE ANALYTICS BOOK CITATION INDEX INDEXED

WEB OF SCIENCE™

Selection of our books indexed in the Book Citation Index in Web of Science™ Core Collection (BKCI)

Interested in publishing with us?
Contact book.department@intechopen.com

Numbers displayed above are based on latest data collected.
For more information visit www.intechopen.com

Chapter 12

Toroidal and Coiled Carbon Nanotubes

Lizhao Liu and Jijun Zhao

Additional information is available at the end of the chapter

http://dx.doi.org/10.5772/51125

1. Introduction

The perfect graphite and carbon nanotube (CNT) are composed of hexagonal rings of carbon atoms. However, non-hexagonal rings like pentagons and heptagons usual exist in the realistic CNT. Due to the change of topology, different arrangements of the pentagons and heptagons would lead to various structures, such as CNTs with Stone-Wales defects [1], CNT junctions [2], toroidal CNTs [3], and coiled CNTs [4, 5]. Each type of these CNT-based structures has its unique physical and chemical properties; as a consequence, the diversity in morphology extends the applications of CNTs. In this chapter, we will review the current progress on two important members of the CNT family, i.e., the toroidal CNTs at the first and coiled CNTs in the second.

The toroidal CNT (also known as carbon nanotorus or carbon nanoring) is a kind of zero-dimensional CNT-based nanostructure. In other words, a carbon nanotorus can be considered as a giant molecule and directly used as a nanoscale device. As for the synthesis of the toroidal CNTs, numerous methods have been proposed, including laser-growth method, ultrasonic treatments, organic reactions, and chemical vapour deposition (CVD), which will be illustrated in the following. In addition to experimental synthesis, various theoretical efforts have been devoted to construct the structural models of the toroidal CNTs. In general, there are two kinds of toroidal CNTs: one is formed by pristine nanotube with pure hexagon networks, and the other contains certain amount of pentagon and heptagon defects. Due to the circular geometry of the carbon nanotorus and incorporation of pentagon/heptagon defects, it may exhibit novel mechanical, electronic and magnetic properties different from the straight CNTs.

Another kind of curved CNT-based nanostructure is the coiled CNT, which is also known as carbon nanocoil or carbon nanospring. Different from the zero-dimensional toroidal CNT, the coiled CNT is a kind of quasi one-dimensional CNT-based nanostructures with a certain spiral

angle. Intuitionally, a carbon nanocoil is like a spring in geometry. Therefore, mechanic properties of the coiled CNTs attract lots of attentions. Among various methods to produce the coiled CNTs, CVD approach is predominant due to the high quality and good controllability. Besides, several methods have been proposed to build the structural models of the coiled CNTs. An important feature of the carbon nanocoil models is the periodic incorporation of pentagons and heptagons in the hexagonal network. In addition, due to the excellent properties of the coiled CNTs, they have promising applications in many fields, such as sensors, electromagnetic nano-transformers or nano-switches, and energy storage devices.

2. Toroidal CNTs

In this section, we summarize experimental fabrication and theoretical modelling of the toroidal CNTs, as well as their physical and chemical properties. The toroidal CNTs are predicted to be both thermodynamic and kinetically stable. Due to the circular geometry, the toroidal CNTs possess excellent properties, especially the electronic and magnetic properties.

2.1. Fabrication

Synthesis and characterization of the toroidal CNTs are of key importance in the carbon nanotorus related fields. Early in 1997, Liu et al. reported synthesis of the toroidal CNTs with typical diameters between 300 and 500 nm by using the laser growth method [3]. From the measurement of scanning force microscopy (SEM) and transmission electron microscopy (TEM), it was shown that the toroidal CNTs were form by single-walled carbon nanotube (SWNT) ropes consisting of 10 to 100 individual nanotubes. Soon after, the toroidal CNTs were also found in the CNT samples prepared by catalytically thermal decomposition of hydrocarbon gas [6] and an ultrasound-aided acid treatment [7, 8]. Later, a variety of experimental approaches were developed to fabricate carbon nanotori, such as organic reactions [9, 10], chemical vapor deposition (CVD) [11, 12], and depositing hydrocarbon films in Tokamak T-10, the facility for magnetic confinement of high-temperature plasma [13]. In addition, incomplete toroidal CNTs [13, 14], large toroidal CNTs with diameters of~200–300 nm, sealed tubular diameters of 50–100 nm [15], and patterning of toroidal CNTs [16, 17] were also achieved in laboratory. In particular, the tubular diameter of a carbon nanotorus is now controllable. Toroidal CNTs from single-walled [7-10, 18, 19], double-walled [20], triple-walled [21], and multi-walled CNTs [6] have been achieved. Combining the experimental measurements and a simple continuum elastic model, formation of the toroidal CNTs was supposed to involve a balance between the tube-tube van der Waals adhesion, the strain energy resulting from the coiling-induced curvature and the strong interaction with the substrate [8, 14]. Various kinds of the toroidal CNTs are presented in Figure 1.

http://dx.doi.org/10.5772/51125

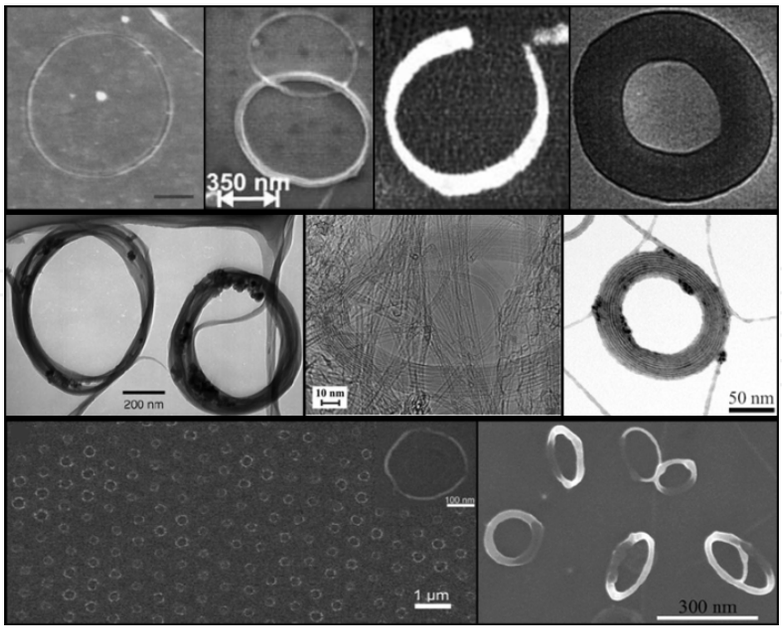

Figure 1. Experimental fabrications of various kinds of toroidal CNTs.

2.2. Structural models and thermodynamic stabilities

Prior to the experimental synthesis, Dunlap proposed to construct the structural model of a carbon nanotorus by connecting two CNTs with different diameters [22]. Almost at the same time, researchers in Japan built a C_{360} nanotorus from C_{60} fullerene [23] and then generated a series of toroidal CNTs with 120 to 1920 carbon atoms using the prescription of Goldberg [24, 25]. So far, there have been six major approaches to construct the structural models of toroidal CNTs: (1) bending a finite CNT and connecting its ends together [26-29]; (2) connecting CNTs with different diameters by introducing pentagons and heptagons [22, 30-32]; (3) constructing from fullerenes [23-25] by employing the prescription of Goldberg [33]; (4) built through the connection of one zigzag-edged chain of hexagons and another armchair-edged chain of hexagons [34]; (5) sewing the walls of a double-walled CNT at both ends [35]; (6) constructing from only pentagons and heptagons [36]. To summarize, there are two kinds of toroidal CNTs: one is formed by pure hexagonal networks and the other is a hexagonal structure with pentagon-heptagon defects. In a more detailed way, Itoh et al. classified the toroidal CNTs into five types using the parameters of the inner (r_i) and outer (r_o) diameters, and the height (h) [37]. As depicted in Figure 2, type (A) indicates a nanotorus with $r_i \approx r_o$, $h \ll r_i$, and $h \approx (r_o - r_i)$, type (B) is the case of $r_i \sim r_o \sim h$ and $h \approx (r_o \circledcirc r_i)$, type (C) denotes $h \ll (r_o \circledcirc r_i)$, type (D) is the case of $r_i < r_o$, $r_o \sim h$, and $h \sim (r_o \circledcirc r_i)$, and type (E) means $(r_o \circledcirc r_i) \ll h$, respectively.

After establishing the structural models, one important issue is to examine the thermodynamic stabilities of the toroidal CNTs. Many groups demonstrated that toroidal CNTs are more stable than C_{60} fullerene through comparing their binding/cohesive energies calculated by means of empirical potential methods [22-25]. Besides, molecular dynamics (MD) simulations also demonstrated that toroidal CNTs can survive under high temperature [23, 29, 38,

39]. Generally, the thermodynamic stability of a carbon nanotorus depends on its geometric parameters, such as ring and tubular diameter, symmetry, curvature, and position of the pentagons and heptagons. Ihara et al. showed that the cohesive energy of a carbon nanotorus derived from C_{60} fullerene decreased with increasing number of carbon atoms in the carbon nanotorus [24]. The ring and tubular diameter can also affect the thermodynamic stability of a carbon nanotorus [40-42]. At a fixed tubular diameter, there was a preferable ring diameter where the nanotorus possesses the lowest formation energy [40]. Besides, dependence of the stability on the rotational symmetry was also reported for the toroidal CNTs [32, 37]. Among the toroidal CNTs constructed from (5, 5), (6, 6), and (7, 7) armchair CNTs, the one with D_{6h} symmetry is energetically favourable [32]. Despite the dependence on the geometric details, it was believed [43, 44] that for the toroidal CNTs with large ring diameters, the pure hexagonal structure is energetically more stable, but for the ones with small ring diameters, the mixture of hexagonal networks and pentagon-heptagon defects is energetically more favourable. In [44], this critical ring diameter is given by the equation $R_c = \pi r^2 Y/(4\sigma)$, where r is the tubular diameter of the initial CNT, Y is the Young's modulus of the initial CNT, and σ is the surface tension of graphite perpendicular to the basal planes. For example, taking the Y = 1.0 TPa, a R_c of 90 nm can be obtained for a carbon nanotorus made of a (10,10) nanotube (r = 0.68 nm).

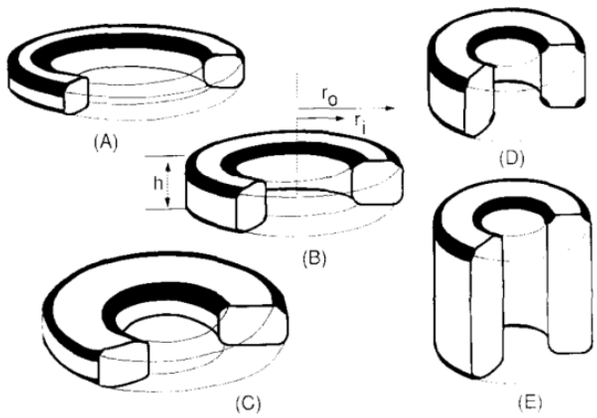

Figure 2. Schematic diagram for five types of toroidal CNTs classified by the parameters of the inner diameter r_i, the outer diameter r_o, and the height h, respectively. Reprinted with permission from [37]. Copyright (1995) Elsevier.

2.3. Mechanical properties

Mechanical property is of fundamental importance for the applications of a material. Employing MD simulation with a reactive force field, Chen et al. investigated the mechanical properties of zero-dimensional nanotorus, one-dimensional nanochain and two-dimensional nanomaile constructed from toroidal CNTs [45]. For a nanotorus constructed from bending a (5, 5) CNT, its Young's modulus increases monotonically with tensile strain from 19.43 to 121.94 GPa without any side constraints and from 124.98 GPa to 1560 GPa with side constraints, respectively, where the side constraint means fixing the position of small regions of

carbon atoms at left and right sides. Besides, the tensile strength of the unconstrained and constrained nanotorus was estimated to be 5.72 and 8.52 GPa, respectively. In addition, the maximum elastic strain is approximate 39% for the nanochain and 25.2% for thenanomaile. For a nanotorus obtained from bending a (10, 10) CNT, its Young's modulus along the tube axis was 913 GPa by taking [46]. Later, buckling behavior of toroidal CNTs under tension was investigated using the molecular mechanics (MM) computations, including the toroidal CNTs formed from (5, 5), (8, 8) and (9, 0) CNTs [47, 48]. It was found that the buckling shapes of the toroidal CNTs constructed from both armchair and zigzag CNTs with an odd number of units are unsymmetrical, whereas those with an even number of units are symmetrical. Recently, reversible elastic transformation between the circular and compressed nanotorus in a colloid has been observed under TEM [17]. This geometric reversibility was also predicted theoretically by using a nonlinear continuum elastic model [49, 50], suggesting the potential application of toroidal CNTs as ultrasensitive force sensors and flexible and stretchable nanodevices.

2.4. Electronic properties

It is well-known that a CNT can be expressed by a chiral vector C_h (n, m) and a translation vector T (p, q) and can be either metallic or semiconducting, depending on its chirality [51]. Since a carbon nanotorus can be considered as a bended CNT or a CNT incorporated with pentagons and heptagons, it would be interesting to explore will the bending behavior or inclusion of pentagons and heptagons affect the electronic properties of the pristine CNT. For a carbon nanotorus formed by bending a (n, m) CNT, it can be divided into three types: (1) if m – n = 3i, and p – q = 3i (i is an integral), the carbon nanotorus is metallic; (2) if m – n = 3i, and p – q ≠ 3i, the carbon nanotorus is semiconducting; (3) if m – n ≠ 3i, and p – q = 3i, the carbon nanotorus is insulating [52]. This classification was partly confirmed by the tight-binding (TB) calculation that a metallic carbon nanotorus can be constructed by bending a metallic CNT and also follows the rule of divisibility by three on the indices of chiral and twisting vectors [53]. Moreover, delocalized and localized deformations play different roles on the electronic properties of a carbon nanotorus built bending a CNT [27]. The delocalized deformations only slightly reduce the electrical conductance, while the localized deformations will dramatically lower the conductance even at relatively small bending angles. Here the delocalized deformation means the deformation induced by the mechanical bending of the CNT, and the localized deformation indicates the deformation induced by the pushing action of the tip of AFM. In addition, Liu et al. reported the oscillation behavior of the energy gap during increasing size of the nanotorus and the gap was eventually converged to that of the infinite CNT [54].

Meanwhile, in the case of incorporation of pentagons and heptagons, a HOMO-LUMO gap can be expected for the carbon nanotorus. For a carbon nanotorus C_{1960} constructed by connecting (6, 6) and (10, 0) CNTs, a gap of 0.05 eV was calculated by a TB approach [44]. Using both the TB and semiempirical quantum chemical approaches, a series of toroidal CNTs with total number of atoms ranging from 120 to 768 were investigated and most of them have HOMO-LUMO gaps [55]. Besides, employing the extended-Hückel method, energy

gaps of 0.4-0.32μB eV were predicted for the toroidal CNTs of C_{170}, C_{250}, C_{360}, C_{520}, and C_{750} [56]. Further accurate DFT examination also showed that the nanotorus C_{444} has a gap of 0.079 eV and the nanotorus C_{672} has a gap of 0.063 eV, respectively [57].

2.5. Magnetic properties

The unique circular geometry endows its advantage to study the magnetic response when ring current flows in a carbon nanotorus. Early in 1997, Haddon predicted that the nanotorus C_{576} has an extremely large and anisotropic ring-current diamagnetic susceptibility, which can be 130 times larger than that of the benzene molecule [58]. Afterwards, colossal paramagnetic moment was also reported in the metallic toroidal CNTs, which was generated by the interplay between the toroidal geometry and the ballistic motion of the π-electrons [28], as shown in Figure 3. For example, the nanotorus C_{1500} built from a (5, 5) CNT possesses a large paramagnetic moment of 88.4 $_{\mu}$B at 0 K. Similarly, the nanotorus C_{1860} built from a (7, 4) CNT has a giant zore-temperature magnetic moment of 98.5 $_{\mu}$B. In addition to the paramagnetic moments, existence of ferromagnetic moments at low temperatures in the toroidal CNTs without heteroatoms was also predicted by using a π-orbital nearest-neighbor TB Hamiltonian with the London approximation, which is attributed to the presence of pentagons and heptagons [59]. Another important phenomenon, i.e., the Aharonov–Bohm effect can be also observed in the toroidal CNTs [60-64]. Indeed, the magnetic properties of the toroidal CNTs are affected by many factors. Liu et al. pointed out that the paramagnetic moments of the toroidal CNTs decrease distinctly as temperature increases [28]. Such temperature dependence was also confirmed by several successive studies [65-68]. Moreover, the magnetic properties of a toroidal CNT also rely on its geometric parameters, such as ring diameter, curvature, chirality, and the arrangement of pentagons and heptagons [65-67].

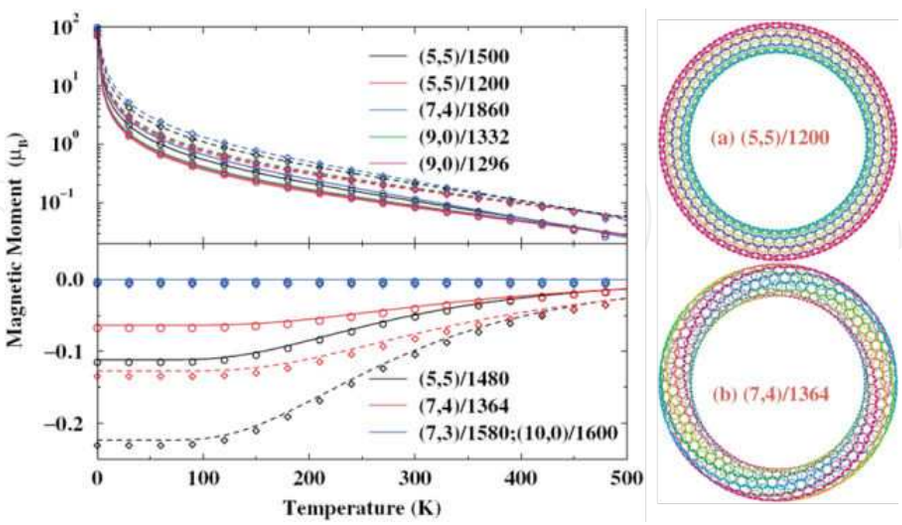

Figure 3. Induced magnetic moment as a function of temperature for various toroidal CNTs in a perpendicular magnetic field of 0.1 T (solid line) and 0.2 T (dashed line), respectively. Reprinted figures with permission from [Liu L, Guo GY, Jayanthi CS, Wu SY. Colossal Paramagnetic Moments in Metallic Carbon Nanotori. 88, 217206 (2002)]. Copyright (2002) by the American Physical Society. http://prl.aps.org/abstract/PRL/v88/i21/e217206.

2.6. Modification of the toroidal CNTs

Chemical modification is an important approach to tailor the properties of materials. A common approach of chemical modification is doping. It was found that doping electrons or holes into a carbon nanotorus could vary its magnetic properties through altering the band-filling configuration [69]. Our previous work also demonstrated that substitutional doping of boron or nitrogen atoms could modify the electronic properties of the toroidal CNTs due to change of the six π-electron orbitals [32]. Moreover, compared with the hexagonal rings, existence of pentagons favours the doping of nitrogen atoms and existence of heptagons prefers the doping of boron atoms. Besides, the toroidal CNTs coated with beryllium can be used as candidates for hydrogen storage. Each beryllium atom can adsorb three H_2 molecules with moderate adsorption energy of 0.2-03 eV/H_2 [70].

Since the toroidal CNTs also have the hollow tubular structures similar to the CNTs, atoms or molecules can be encapsulated into the toroidal CNTs. Early in 2007, Hilder et al. examined the motion of a single offset atom and a C_{60} fullerene inside a carbon nanotorus to explore its application as high frequency nanoscale oscillator [71]. They demonstrated that the C_{60} fullerene encapsulated carbon nanotorus can create high frequency up to 150 GHz, which may be controlled by changing the orbiting position. By inserting the chains of Fe, Au, and Cu atoms into a carbon nanotorus, Lusk et al. investigated the geometry, stability and electronic magnetic properties of this nano-composite structure [72]. Reduced HOMO-LUMO gap and ferromagnetism of the nanotorus were predicted by encapsulating chains of metal atoms. In addition, diffusion behavior of water molecules forming two oppositely polarized chains in a carbon nanotorus was studied by MD simulations. It was demonstrated that Fickian diffusion is in the case of a single chain and the diffusion for two or more chains is consistent with single-file diffusion [73].

3. Coiled carbon nanotube

Similar to the case of the toroidal CNTs, we first introduce the experimental synthesis and theoretical methods to construct the structural models, as well as their formation mechanism and stabilities. Then the mechanic properties and electronic properties of the coiled CNTs are summarized. Finally, the promising applications of coiled CNTs in various fields compared with their straight counterparts owing to their spiral geometry and excellent properties will be discussed in the end of this section.

3.1. Fabrication and formation mechanism

The coiled CNTs were first experimentally produced through catalytic decomposition of acetylene over silica-supported Co catalyst at 700 °C in 1994 [4, 5]. Afterwards, numerous methods have been proposed to synthesize the coiled CNTs, including the laser evaporation of the fullerene/Ni particle mixture in vacuum [74], opposed flow flame combustion of the fuel and the oxidizer streams [75], electrolysis of graphite in fused NaCl at 810 °C [76], self-assembly from π-conjugated building blocks [77, 78], and CVD method [79-83]. Among

these various methods, the CVD approach is predominant due to its high quality, which has been reviewed by several literatures [84-86]. To fabricate the coiled CNTs, CVD process involves the pyrolysis of a hydrocarbon (e.g. methane, acetylene, benzene, propane) over transition-metal catalysts (e.g. Fe, Co, Ni) at high temperatures. Compared to the high growth temperature (> 2000 °C) of CNT through arc discharge and laser evaporation process, the relatively low growth temperature of CVD method (500–1000 °C) allows carbon atoms move slowly and form non-hexagonal carbon rings [84]. In 2006, Lau et al. reviewed the three major CVD-based methods to fabricate the coiled CNTs, including the catalyst supported CVD growth, on substrate CVD growth and template-based CVD growth [84]. Later, synthetic parameters of CVD growth of the coiled CNTs, such as catalyst, gas atmosphere and temperature, were introduced and catalogued by Fejes et al. [85] and Shaikjee et al. [86], respectively. Moreover, Shaikjee et al. [86] presented different types of the coiled CNTs with non-linear morphology, which are shown in Figure 4.

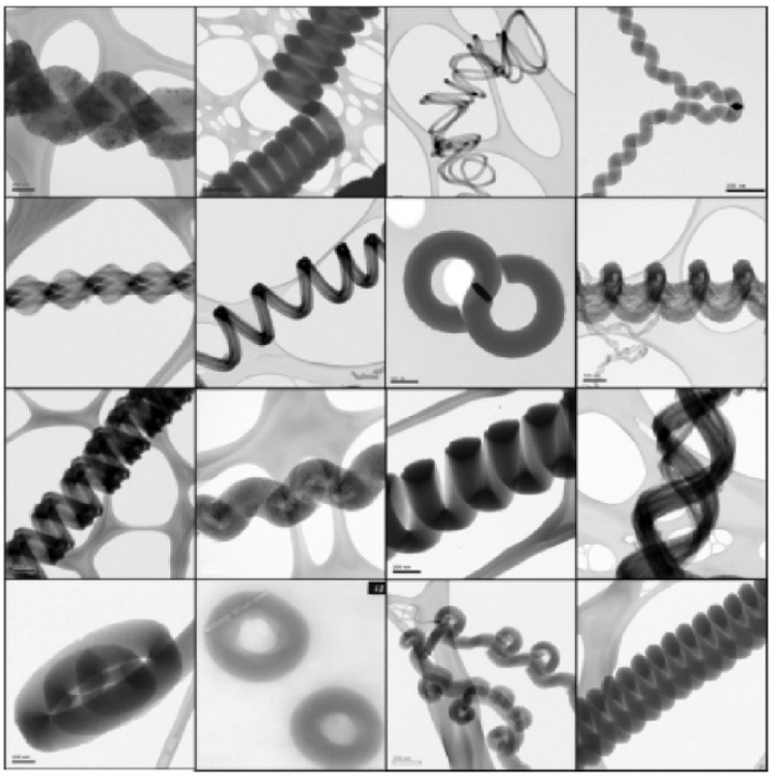

Figure 4. Experimental fabrications of various kinds of the coiled CNTs. Reprinted with permission from [86]. Copyright (2011) Elsevier.

As for the formation mechanism of the coiled CNTs, Fonseca et al. presented a formation of (chiral and achiral) knees on a catalyst particle to further form toroidal and coiled CNTs, which can be described by a simple formalism using the heptagon-pentagon construction [87]. In addition, formation of the coiled CNTs is closely related to the catalyst. Pan et al. suggested that the catalyst grain is crucial to the geometry of a carbon nanocoil and the non-uniformity of carbon extrusion speed in the different parts of the catalyst grain leads to the

helical growth of the coiled CNTs [88]. Chen et al. pointed out that the driving force of coiling straight CNTs was the strong catalytic anisotropy of carbon deposition between different crystal faces [89]. For growth of carbon microcoils, the catalyst grain rotates around the coil axis which is on the symmetric face of the deposition faces; while for the twisted carbon nanocoils, the catalyst grain rotates around the axis which is perpendicular to the symmetric face of the deposition faces. Taking both the energy and entropy into account, Bandaru et al. proposed a mechanism that for a given volume of material, the helical form occupies the least amount of space and the entropy of the ambient conditions should increase to compensate for the close packing of the helices, which in turn is facilitated by nonwetting catalyst particles or induced by catalyst/ambient agitation in the CVD growth [90].

3.2. Structural models and thermodynamic stabilities

An important feature of a carbon nanocoil is incorporation of pentagons and heptagons in the hexagonal network. Dunlap [22, 91] showed that connecting two CNTs with pentagons and heptagons could result in a curved structure or knee structure. Based on the knee structure, Fonseca et al. was able to construct the toroidal and coiled CNTs using the knee segments as building blocks, where the former is an in-plane structure and the latter is out of plane [92]. In addition, researchers in Japan proposed two kinds of methods to construct structures of the coiled CNTs. One approach is to cut the toroidal CNTs into small pieces and recombine them to form the coiled CNTs with one pitch containing one nanotorus [37, 93]. For the coiled CNTs built from toroidal segments, Setton et al. suggested that the toroidal segments were only feasible for single-shell or at best two-shell nanocoils [94]. The other way is to insert pentagons and heptagons into a perfect graphene network and then roll up this structure to form a carbon nanocoil [95, 96]. Similarly, Biró et al. proposed to build the coiled CNTs from rolling up the Haeckelite structure, a graphite sheet composed of polygonal rings [97]. Recently, we were able to construct the carbon nanocoils from segment of CNTs in which the tube chirality is maintained [98]. Through introducing a pair of pentagons in the outer side and another pair of heptagons in the inner side into the segment of an armchair CNT, a curved structure can be obtained. Using this curved structure as a building block, a carbon nanocoil can be formed by connecting the building blocks with a rotate angle. This method was also employed to construct the structural models of the toroidal CNTs, as mentioned above [32]. A simple schematic diagram of this method is presented in Figure 5. Usually, a carbon nanocoil can be expressed by the parameters of inner coil diameter (D_i), outer coil diameter (D_o), tubular diameter (D_t) and coil pitch (λ) [84, 86], as illustrated in Figure 6.

In addition to the structural models of the coiled CNTs, several works have been devoted to investigating their thermodynamic stabilities. Employing MD simulation, Ihara et al. [93] obtained the cohesive energies of 7.41, 7.39 and 7.43 eV/atom for C_{360}, C_{540} and C_{1080} nanocoils, respectively, which are close to that of graphite sheet (7.44 eV/atom) and lower than that of the C_{60} fullerene (7.29 eV/atom). Therefore, these carbon nanocoils are more stable than C_{60} fullerene. Moreover, these carbon nanocoils can maintain the coiled geometry without collapse at a temperature up to 1500 K, which further confirms their thermodynamical

stability. By taking into account the volume free energy, the surface energy, and the curvature elastic energy, it was found that there is a threshold condition for the formation of straight multiwall CNTs [99]. Below that the straight multiwall CNTs become unstable and would undergo a shape deformation to form the coiled CNTs.

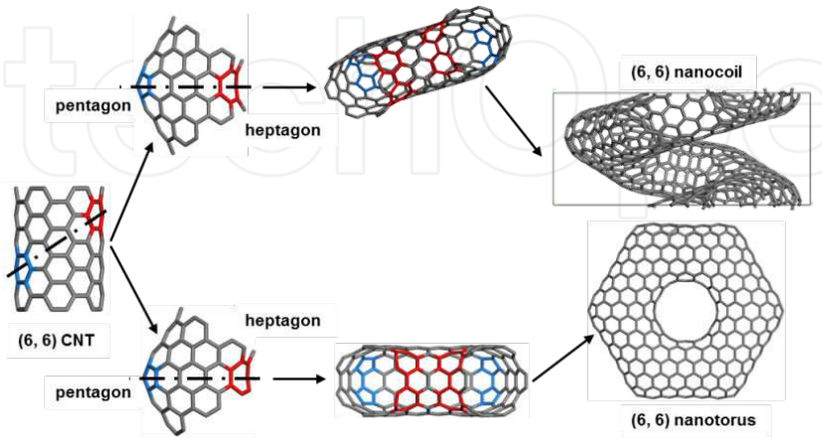

Figure 5. Schematic diagram for constructing the structural models of (6, 6) carbon nanotorus and nanocoil by introducing pairs of pentagons (highlighted in blue) and heptagons (highlighted in red).

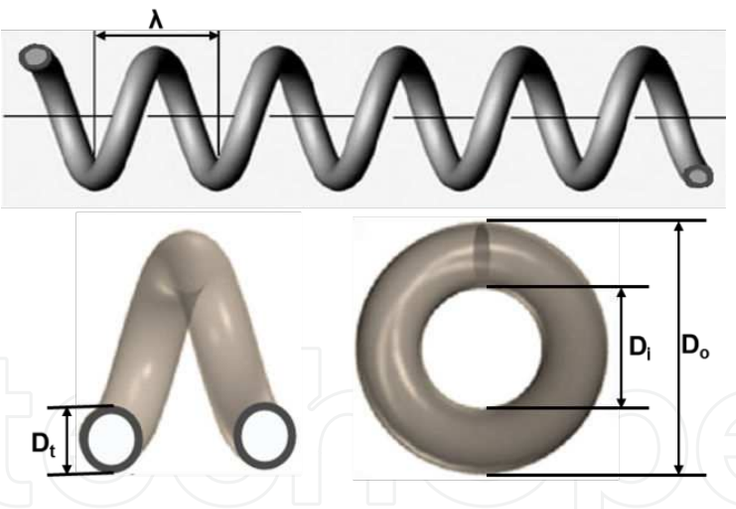

Figure 6. Parameters of inner coil diameter D_i, outer coil diameter D_o, tubular diameter D_t and coil pitch λ to describe a carbon nanocoil.

3.3. Mechanical properties

Intuitively, a carbon nanocoil is similar to a spring in geometry. It is well-known that spring exhibits excellent mechanic properties and is very useful in the mechanics-based devices. Therefore, mechanical properties of the coiled CNTs as "nanospring" have attracted lots of attentions. Early in 2000, Volodin et al. measured the elastic properties of the coiled CNTs with atomic force microscopy (AFM) and showed that the coiled CNTs with coil diameters

http://dx.doi.org/10.5772/51125

(> 170 nm) possess high Young's modulus of 0.4–0.9 TPa [100]. Using a manipulator-equipped SEM, Hayashida reported the Young's modulus of 0.04–0.13 TPa and the elastic spring constants of 0.01–0.6 N/m for the coiled CNTs with coil diameters ranging from 144 to 830 nm [101]. Remarkable spring-like behavior of an individual carbon nanocoil has been demonstrated by Chen et al. [102], as presented in Figure 7. A spring constant of 0.12 N/m in the low-strain regime and a maximum elastic elongation of 33% were obtained from AFM measurement. In contrast to the high measured Young's modulus, the shear modulus of the coiled CNTs is extremely low. Chen et al. [102] considered the coiled CNTs with a D_o of ~126±4 nm but different D_i. For the case of $D_i = 3/4\ D_o$, a shear modulus of ~2.5±0.4 GPa was estimated; if $D_i = 1/2\ D_o$, the corresponding shear modulus was ~2.3±0.4 GPa; and if $D_i = 0$, a shear modulus of ~2.1±0.3 GPa can be obtained. Afterwards, Huang [103] studied the coiled CNTs under uniaxial tension in simple explicit expressions and obtained a maximum elastic elongation of ~30%, a shear modulus of 2.8–3.4 GPa and a spring constant of ~0.1–0.4 N/m for the double nanocoils formed by twisting two single nanocoils, which is comparable to the experimental result [102]. Later, Chang et al. reported a shear modulus of 3±0.2 GPa for the double coiled CNTs [104]. In addition, Poggi et al. demonstrated the compression behavior of the coiled CNTs and presented that repeated compression/buckling/decompression of the nanocoil was very reproducible with a limiting compression of 400 nm [105].

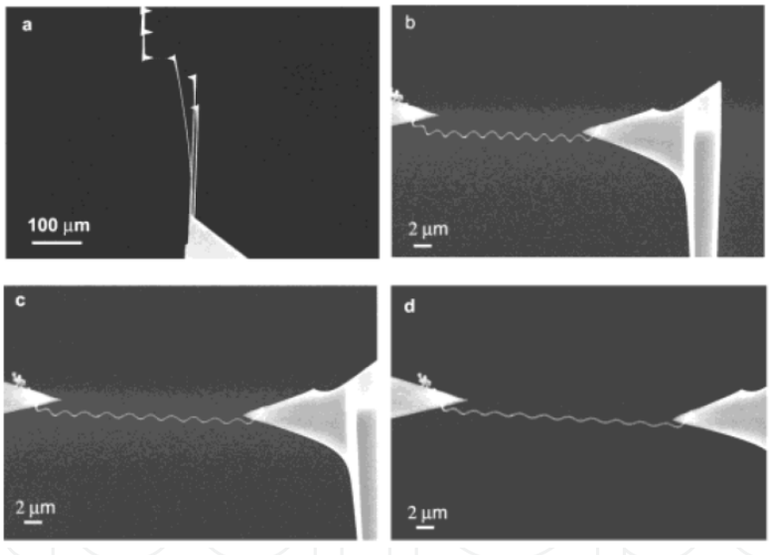

Figure 7. Measurement of the mechanical properties of a carbon nanocoil using the AFM cantilevers: (b) the initial state, (c) at a tensile strain of 20%, and (d) at a tensile strain of 33%. Reprinted with permission from [102]. Copyright (2003) American Chemical Society.

In addition to the experimental measurements, numerous theoretical simulations were carried out to investigate the mechanical properties of the coiled CNTs. Using the Kirchhoff rod model, Fonseca et al. derived a series of expressions to obtain the Young's modulus and Poisson's ratios for the coiled CNTs. Taking the parameters for the carbon nanocoil reported by Chen et al. [102], Fonseca et al. estimated the Young's modulus of 6.88 GPa for a nanocoil with a coil diameter of 120 nm, a Poisson's ratio of 0.27 and a shear modulus of 2.5 GPa [106,

107]. Besides, equations were derived to calculate the elastic constants of the forests of the coiled CNTs, which shows that the entanglement among neighboring nanocoils will contribute to the mechanical properties of the nanocoil forests [108]. Employing the DFT and TB calculations, we computed the Young's modulus and elastic constant of a series of single-walled carbon nanocoils built from the armchair CNTs [98]. The Young's modulus ranges from 3.43 to 5.40 GPa, in good agreement with the Fonseca's reports [106, 107] and the elastic constant lies between 15.37 to 44.36 N/m, higher than the experimental values [100, 102]. Furthermore, superelastic behavior of the coiled CNTs was also predicted from our computations where the coiled CNTs can undertake an elastically tensile strain up to ~60% and compressive strain up to ~20–35%. Such superelasticity is due to the invariance of bond length under strain associated with the strong covalent C-C bonding. In a recent computation on the mechanic properties of the single-walled carbon nanocoils using the finite element ANSYS code, spring constants ranging from 15–30 N/m were obtained for the armchair carbon nanocoils with different tubular diameters [109]. As the tubular diameter increases, the spring constant increases accordingly. Generally speaking, the calculated Young's modulus and elastic constants for the coiled CNTs are more or less different from that of the experimental measurements. This difference may be attributed to the structural details of the synthesized carbon nanocoils, especially the larger sizes of experimental nanocoil samples.

3.4. Electronic and transport properties

Similar to the toroidal CNTs, pentagons and heptagons exist in the coiled CNTs, which may lead to different electric properties with regard to that of the pristine CNTs. Using the two and four probes methods, Kaneto et al. measured the electric conductivity of the micro carbon nanocoils, which lies in 30–100 S/cm [110]. Later, it was found that for a carbon nanocoil with a coil diameter of 196 nm and a length of 1.5 mm, the conductivity is about 180 S/cm [101], which is much smaller than a straight CNT (~10^4 S/cm) [111]. Recently, Chiu et al. reported a very high conductivity of 2500 S/cm and an electron hopping length of ~5 nm for the single carbon nanocoils measured at low temperature [112]. An even higher electron hopping length of 5–50 nm was predicted by Tang et al. [113]. Moreover, the temperature dependence of the electric resistance was also observed where resistivity of the carbon nanocoil decreases as the annealing temperature increases [114]. Therefore, the measured electric properties of the coiled CNTs are closely related to the temperature and details of the samples.

Theoretically, employing a simple TB model, Akagi et al. [95, 96] calculated the band structures and electron density of states of the carbon nanocoils and suggested that the coiled CNTs could be metallic, semiconducting and semimetallic, depending on the arrangement of the pentagons and heptagons. Compared with the pristine CNTs, the semimetal property is unique for the carbon nanocoil [96]. Recently, we investigated the electric conductance of a series of armchair carbon nanocoils through using a π-orbital TB model combined with the Green's function approach [115]. Using the metallic armchair CNTs as the electrodes, we calculated the quantum conductance of the (5, 5), (6, 6) and (7, 7) carbon nanocoils, as presented in Figure 8. Clearly, there is a transport gap in the conductance spectrum. Further

analysis of the electronic states indicates that only incorporation of pentagons and heptagons (such as Stone-Wales defects) can not lead to gap opening, and thus creation of the band gap should be attributed to the existence of sp^3 C-C bonds caused by coiling the CNTs. In addition, change of quantum conductance for the armchair carbon nanocoils under uniaxial elongation or compression is not distinct due to the nearly invariant bond length under strain, i.e. superelasticity [98].

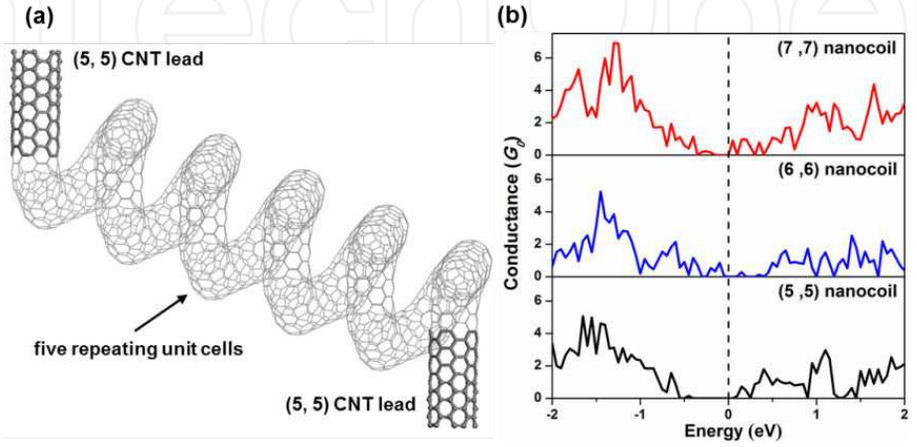

Figure 8. Structural model to calculate conductance of the (5, 5) carbon nanocoil (a) and conductance of the (5, 5), (6, 6) and (7, 7) carbon nanocoils (b). Reprinted with permission from [115]. Copyright (2011) Science China Press and Springer-Verlag Berlin Heidelberg.

3.5. Applications

Owing to the spiral geometry and unusual properties, the coiled CNTs have promising applications in various fields compared with their straight counterparts [84-86, 116]. One important application of the carbon nanocoils is to act as the sensors. In 2004, Volodin et al. [117] reported the use of coiled nanotubes as self-sensing mechanical resonators, which is able to detect fundamental resonances ranging from 100 to 400 MHz, as illustrated in Figure 9. The self-sensing carbon nanocoil sensors are sensitive to mass change and well suited for measuring small forces and masses in the femtogram range. After measuring the mechanical response of the coiled CNTs under compression using AFM, Poggi et al. pointed out that a nonlinear response of the carbon nanocoil can be observed, which is associated with compression and buckling of the nanocoil [105]. Bell et al. demonstrated that the coiled CNTs can be used as high-resolution force sensors in conjunction with visual displacement measurement as well as electromechanical sensors due to the piezoresistive behavior without an additional metal layer [118]. Besides, the applications of carbon nanocoils as magnetic sensors [119], tactile sensors [120], and gas sensors [121] were also exploited.

Another kind of major applications of the carbon nanocoils is to form composites with other materials. It was found that incorporation of carbon nanocoils in epoxy nanocomposites can enhance the mechanic properties of the epoxy nanocomposites [122-125]. Besides, the coiled CNT/silicone–rubber composites show high resistive sensitivity, relying on the densi-

ty of the carbon nanocoil [126, 127]. In addition, metal-coated carbon nanocoils can also display some properties different from the pristine coiled CNTs. Tungsten-containing carbon nanocoils can expand and contract as flexibly as macro-scale springs and the elastic constants of the tungsten-containing carbon nanocoils rises along with increasing content of tungsten [128]. Bi et al. [129] found that the coiled CNTs coated with Ni have enhanced microwave absorption than the uncoated ones, which is results from stronger dielectric and magnetic losses.

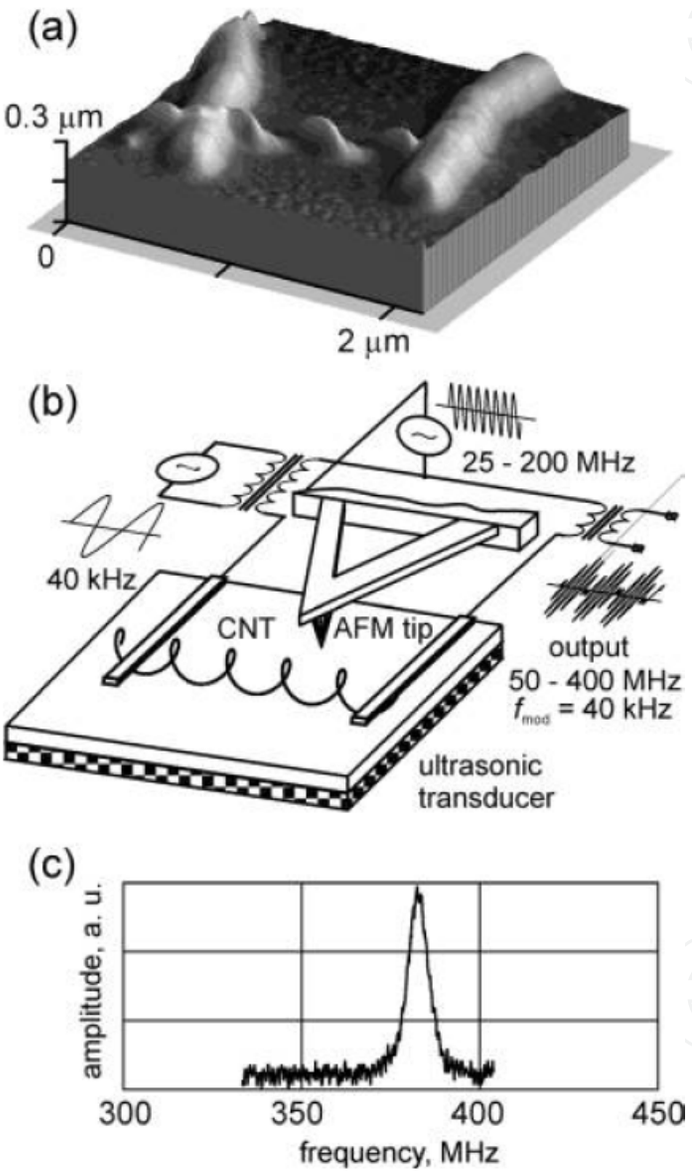

Figure 9. The carbon nanocoil to act as a mechanical resonator: (a) AFM image of the carbon nanocoil, (b) circuit contains two broad-band radio frequency transformers and the carbon nanocoil, and (c) resonant response of the carbon nanocoil device to electromechanical excitation. Reprinted with permission from [117]. Copyright (2004) American Chemical Society.

In addition, field emission [79, 130], energy storage [131, 132] and biological applications [133] of the coiled CNTs were also reported. Nowadays, the coiled CNT have been used as

sensors [117-121], flat panel field emission display [79], microwave absorbers [134] and additives in the cosmetic industry [86].

4. Conclusion

Experimental fabrication and theoretical modelling of the toroidal and coiled CNTs were reviewed in this chapter. Compared with the pristine CNTs, the zero-dimensional toroidal CNTs exhibit excellent electromagnetic properties, such as persistent current and Aharonov–Bohm effect. Moreover, electronic properties of the toroidal CNTs can be tuned by chemical modification. In contrast to the toroidal CNTs, the coiled CNTs are quasi one-dimensional CNT-based nanostructures. Due to the spring-like geometry, the coiled CNTs possess fascinating mechanical properties, which are known as superelastic properties. This superelasticity allows the carbon nanocoils to act as electromechanical, electromagnetic, and chemical sensors. In addition, the coiled CNTs have been used commercially to fabricate flat panel field emission display, microwave absorbers and cosmetics.

As mentioned above, the toroidal CNTs synthesized experimentally are usually formed by the bundle of single-walled CNTs and have large ring diameters. Therefore, fabrications of the single-walled toroidal CNTs, as well as the toroidal CNTs of controllable ring diameters, are great challenges. Moreover, achievement of inserting atoms/molecules into the toroidal CNTs is another key issue under solution. On the other hand, since the formation mechanism of the coiled CNTs depends closely on the catalysts, searching for the optimal catalysts is significant for the quality and quantity of the nanocoil samples. Besides, finding appropriate geometry and concentration of the coiled CNTs is also necessary to improve performance of nanocomposites with the carbon nanocoils. Further experimental and theoretical works are expected to carry out to solve these problems.

Acknowledgements

This work was supported by the National Natural Science Foundation of China (No. 11174045, No. 11134005).

Author details

Lizhao Liu and Jijun Zhao*

*Address all correspondence to: zhaojj@dlut.edu.cn

Key Laboratory of Materials Modification by Laser, Ion and Electron Beams (Dalian University of Technology), Ministry of Education, Dalian 116024, China

References

[1] hang, P., Lammert, P. E., & Crespi, V. H. (1998). Plastic Deformations of Carbon Nanotubes. *Physical Review Letters*, 81(24), 5346-5349.

[2] Yao, Z., Postma, H. W. C., Balents, L., & Dekker, C. (1999). Carbon nanotube intramolecular junctions. *Nature*, 402(6759), 273-276.

[3] Liu, J., Dai, H. J., Hafner, J. H., Colbert, D. T., Smalley, R. E., Tans, S. J., & Dekker, C. (1997). Fullerene'crop circles. *Nature*, 385(6619), 780-781.

[4] Amelinckx, S., Zhang, X. B., Bernaerts, D., Zhang, X. F., Ivanov, V., & Nagy, J. B. (1994). A Formation Mechanism for Catalytically Grown Helix-Shaped Graphite Nanotubes. *Science*, 265(5172), 635-639.

[5] Zhang, X. B., Zhang, X. F., Bernaerts, D., Tendeloo, G. v., Amelinckx, S., Landuyt, J. v., Ivanov, V., Nagy, J. B., Ph, L., & Lucas, A. A. (1994). The Texture of Catalytically Grown Coil-Shaped Carbon Nanotubules. *Europhysics Letters*, 27(2), 141-146.

[6] Ahlskog, M., Seynaeve, E., Vullers, R. J. M., Van Haesendonck, C., Fonseca, A., Hernadi, K. B., & Nagy, J. (1999). Ring formations from catalytically synthesized carbon nanotubes. *Chemical Physics Letters*, 202.

[7] Martel, R., Shea, H. R., & Avouris, P. (1999). Rings of single-walled carbon nanotubes. *Nature*, 398(6725), 299.

[8] Martel, R., Shea, H. R., & Avouris, P. (1999). Ring Formation in Single-Wall Carbon Nanotubes. *The Journal of Physical Chemistry B*, 103(36), 7551-7556.

[9] Sano, M., Kamino, A., Okamura, J., & Shinkai, S. (2001). Ring Closure of Carbon Nanotubes. *Science*, 293(5533), 1299-1301.

[10] Geng, J., Ko, Y. K., Youn, S. C., Kim, Y. H., Kim, S. A., Jung, D. H., & Jung, H. T. (2008). Synthesis of SWNT Rings by Noncovalent Hybridization of Porphyrins and Single-Walled Carbon Nanotubes. *The Journal of Physical Chemistry C*, 112(32), 12264-12271.

[11] Song, L., Ci, L. J., Sun, L. F., Jin, C., Liu, L., Liu, W., Zhao, D., Luo, X., Zhang, S., Xiang, Z., Zhou, Y., Zhou, J., Ding, W., Wang, Y., , Z. L., & Xie, S. (2006). Large-Scale Synthesis of Rings of Bundled Single-Walled Carbon Nanotubes by Floating Chemical Vapor Deposition. *Advanced Materials*, 18(14), 1817-1821.

[12] Zhou, Z., Wan, D., Bai, Y., Dou, X., Song, L., Zhou, W., Mo, Y., & Xie, S. (2006). Ring formation from the direct floating catalytic chemical vapor deposition. *Physica E: Low-dimensional Systems and Nanostructures*, 33(1), 24-27.

[13] Kukushkin, A. B., Neverov, V. S., Marusov, N. L., Semenov, I. B., Kolbasov, B. N., Voloshinov, V. V., Afanasiev, A. P., Tarasov, A. S., Stankevich, V. G., Svechnikov, N. Y., Veligzhanin, A. A., Zubavichus, Y. V., & Chernozatonskii, L. A. (2011). Few-nano-

meter-wide carbon toroids in the hydrocarbon films deposited in tokamak T-10. *Chemical Physics Letters*, 265 -268 .

[14] Wang, X., Wang, Z., Liu, Yq., Wang, C., Bai, C., & Zhu, D. (2001). Ring formation and fracture of a carbon nanotube. *Chemical Physics Letters*, 339(1-2), 36 -40.

[15] Lyn, M. E., He, J., & Koplitz, B. (2005). Laser-induced production of large carbon-based toroids. *Applied Surface Science*, 246(1-3), 44-47.

[16] Motavas, S., Omrane, B., & Papadopoulos, C. (2009). Large-Area Patterning of Carbon Nanotube Ring Arrays. *Langmuir*, 25(8), 4655-4658.

[17] Chen, L., Wang, H., Xu, J., Shen, X., Yao, L., Zhu, L., Zeng, Z., Zhang, H., & Chen, H. (2011). Controlling Reversible Elastic Deformation of Carbon Nanotube Rings. *Journal of the American Chemical Society*, 133(25), 9654-9657.

[18] Komatsu, N., Shimawaki, T., Aonuma, S., & Kimura, T. (2006). Ultrasonic isolation of toroidal aggregates of single-walled carbon nanotubes. *Carbon*, 44(10), 2091-2093.

[19] Guo, A., Fu, Y., Guan, L., Zhang, Z., Wu, W., Chen, J., Shi, Z., Gu, Z., Huang, R., & Zhang, X. (2007). Spontaneously Formed Closed Rings of Single-Wall Carbon Nanotube Bundles and Their Physical Mechanism. *The Journal of Physical Chemistry C*, 111(9), 3555-3559.

[20] Colomer, J. F., Henrard, L., Flahaut, E., Van Tendeloo, G., Lucas, A. A., & Lambin, P. (2003). Rings of Double-Walled Carbon Nanotube Bundles. *Nano Letters*, 3(5), 685-689.

[21] Yu, H., Zhang, Q., Luo, G., & Wei, F. (2006). Rings of triple-walled carbon nanotube bundles. *Applied Physics Letters*, 89(22), 223106.

[22] Dunlap, B. I. (1992). Connecting carbon tubules. *Physical Review B*, 46(3), 1933-1936.

[23] Itoh, S., Ihara, S., & Kitakami, J. I. (1993). Toroidal form of carbon C_{360}. *Physical Review B*, 47(3), 1703-1704.

[24] Ihara, S., Itoh, S., & Kitakami, J. I. (1993). Toroidal forms of graphitic carbon. *Physical Review B*, 47(19), 12908-12911.

[25] Itoh, S., & Ihara, S. (1993). Toroidal forms of graphitic carbon II. Elongated tori. *Physical Review B*, 48(11), 8323-8328.

[26] Kirby, E. C., Mallion, R. B., & Pollak, P. (1993). Toroidal polyhexes. *Journal of the Chemical Society, Faraday Transactions*, 89(12), 1945-1953.

[27] Liu, L., Jayanthi, C. S., & Wu, S. Y. . (2001). Structural and electronic properties of a carbon nanotorus: Effects of delocalized and localized deformations. *Physical Review B*, 64(3), 033412 .

[28] Liu, L., Guo, G. Y., Jayanthi, C. S., & Wu, S. Y. (2002). Colossal Paramagnetic Moments in Metallic Carbon Nanotori. *Physical Review Letters*, 88(21), 217206 .

[29] Hod, O., Rabani, E., & Baer, R. (2003). Carbon nanotube closed-ring structures. *Physical Review B*, 67(19), 195408.

[30] Cox, B. J., & Hill, J. M. (2007). New Carbon Molecules in the Form of Elbow-Connected Nanotori. *The Journal of Physical Chemistry C*, 111(29), 10855-10860.

[31] Baowan, D., Cox, B. J., & Hill, J. M. (2008). Toroidal molecules formed from three distinct carbon nanotubes. *Journal of Mathematical Chemistry*, 44(2), 515-527.

[32] Liu, L., Zhang, L., Gao, H., & Zhao, J. (2011). Structure, energetics, and heteroatom doping of armchair carbon nanotori. *Carbon*, 49(13), 4518-4523.

[33] Klein, D. J., Seitz, W. A., & Schmalz, T. G. (1986). Icosahedral symmetry carbon cage molecules. *Nature*, 323(6090), 703-706.

[34] Itoh, S., & Ihara, S. (1994). Isomers of the toroidal forms of graphitic carbon. *Physical Review B*, 49(19), 13970-13974.

[35] Nagy, C., Nagy, K., & Diudea, M. (2009). Elongated tori from armchair DWNT. *Journal of Mathematical Chemistry*, 45(2), 452-459.

[36] László, I., & Rassat, A. (2001). Toroidal and spherical fullerene-like molecules with only pentagonal and heptagonal faces. *International Journal of Quantum Chemistry*, 84(1), 136-139.

[37] Ihara, S., & Itoh, S. (1995). Helically coiled and toroidal cage forms of graphitic carbon. *Carbon*, 33(7), 931-939.

[38] Taşcı, E., Yazgan, E., Malcıoğlu, O. B., & Erkoç, Ş. (2005). Stability of Carbon Nanotori under Heat Treatment: Molecular-Dynamics Simulations. *Fullerenes, Nanotubes and Carbon Nanostructures*, 13(2), 147-154.

[39] Chen, C., Chang, J. G., Ju, S. P., & Hwang, C. C. (2011). Thermal stability and morphological variation of carbon nanorings of different radii during the temperature elevating process: a molecular dynamics simulation study. *Journal of Nanoparticle Research*, 13(5), 1995-2006.

[40] Yang, L., Chen, J., & Dong, J. (2004). Stability of single-wall carbon nanotube tori. *Physica Status Solidi (b)*, 241(6), 1269-1273.

[41] Feng, C., & Liew, K. M. (2009). Energetics and structures of carbon nanorings. *Carbon.*, 47(7), 1664-1669.

[42] Liu, P., Zhang, Y. W., & Lu, C. . (2005). Structures and stability of defect-free multiwalled carbon toroidal rings. *Journal of Applied Physics*, 113522 .

[43] Han, J. (1998). Energetics and structures of fullerene crop circles. *Chemical Physics Letters*, 282(2), 187-191.

[44] Meunier, V., Lambin, P., & Lucas, A. A. (1998). Atomic and electronic structures of large and small carbon tori. *Physical Review B*, 57(23), 14886-14890.

[45] Chen, N., Lusk, M. T., van Duin, A. C. T., & Goddard, W. A. I. I. I. (2005). Mechanical properties of connected carbon nanorings via molecular dynamics simulation. *Physical Review B*, 72(8), 085416.

[46] Çağin, T., Gao, G., & Goddard, I. I. I. W. A. (2006). Computational studies on mechanical properties of carbon nanotori. *Turkish Journal of Physics*, 30(4), 221-229.

[47] Feng, C., & Liew, K. M. (2009). A molecular mechanics analysis of the buckling behavior of carbon nanorings under tension. *Carbon*, 47(15), 3508-3514.

[48] Feng, C., & Liew, K. M. (2010). Buckling Behavior of Armchair and Zigzag Carbon Nanorings. *Journal of Computational and Theoretical Nanoscience*, 7(10), 2049-2053.

[49] Zheng, M., & Ke, C. (2010). Elastic Deformation of Carbon-Nanotube Nanorings. *Small*, 6(15), 1647-1655.

[50] Zheng, M., & Ke, C. (2011). Mechanical deformation of carbon nanotube nano-rings on flat substrate. *Journal of Applied Physics*, 109(7), 074304-074310.

[51] Saito, R., Dresselhaus, G., & Dresselhaus, M. S. (1998). Physical properties of carbon nanotubes. London, Imperial College Press.

[52] Zhenhua, Z., Zhongqin, Y., Xun, W., Jianhui, Y., Hua, Z., Ming, Q., & Jingcui, P. (2005). The electronic structure of a deformed chiral carbon nanotorus. *Journal of Physics: Condensed Matter*, 17(26), 4111-4120.

[53] Ceulemans, A., Chibotaru, L. F., Bovin, S. A., & Fowler, P. W. (2000). The electronic structure of polyhex carbon tori. *The Journal of Chemical Physics*, 112(9), 4271-4278.

[54] Liu, C. P., & Ding, J. W. (2006). Electronic structure of carbon nanotori: the roles of curvature, hybridization, and disorder. *Journal of Physics Condensed Matter*, 18(16), 4077-4084.

[55] Oh, D. H., Mee, Park. J., & Kim, K. S. (2000). Structures and electronic properties of small carbon nanotube tori. *Physical Review B*, 62(3), 1600-1603.

[56] Yazgan, E., Taşci, E., Malcioğlu, O. B., & Erkoç, Ş. (2004). Electronic properties of carbon nanotoroidal structures. *Journal of Molecular Structure: THEOCHEM*, 681(1-3), 231-234.

[57] Wu, X., Zhou, R., Yang, J., & Zeng, X. C. (2011). Density-Functional Theory Studies of Step-Kinked Carbon Nanotubes. *The Journal of Physical Chemistry C*, 115(10), 4235-4239.

[58] Haddon, R. C. (1997). Electronic properties of carbon toroids. *Nature*, 388(6637), 31-32.

[59] Rodríguez-Manzo, J. A., López-Urías, F., Terrones, M., & Terrones, H. (2004). Magnetism in Corrugated Carbon Nanotori: The Importance of Symmetry, Defects, and Negative Curvature. *Nano Letters*, 4(11), 2179-2183.

[60] Lin, M. F., & Chuu, D. S. (1998). Persistent currents in toroidal carbon nanotubes. *Physical Review B*, 57(11), 6731-6737.

[61] Latil, S., Roche, S., & Rubio, A. (2003). Persistent currents in carbon nanotube based rings. *Physical Review B*, 67(16), 165420.

[62] Shyu, F. L., Tsai, C. C., Chang, C. P., Chen, R. B., & Lin, M. F. (2004). Magnetoelectronic states of carbon toroids. *Carbon*, 42(14), 2879-2885.

[63] Margańska, M., Szopa, M., & Zipper, E. (2005). Aharonov-Bohm effect in carbon nanotubes and tori. *Physica Status Solidi (b)*, 242(2), 285-290.

[64] Zhang, Z. H., Yuan, J. H., Qiu, M., Peng, J. C., & Xiao, F. L. (2006). Persistent currents in carbon nanotori: Effects of structure deformations and chirality. *Journal of Applied Physics*, 99(10), 104311 .

[65] Tsai, C. C., Shyu, F. L., Chiu, C. W., Chang, C. P., Chen, R. B., & Lin, M. F. (2004). Magnetization of armchair carbon tori. *Physical Review B*, 70(7), 075411.

[66] Liu, C. P., Chen, H. B., & Ding, J. W. (2008). Magnetic response of carbon nanotori: the importance of curvature and disorder. *Journal of Physics: Condensed Matter*, 20(1), 015206.

[67] Liu, C. P., & Xu, N. (2008). Magnetic response of chiral carbon nanotori: The dependence of torus radius. *Physica B: Condensed Matter*, 403(17), 2884-2887.

[68] Zhang, Z., & Li, Q. (2010). Combined Effects of the Structural Deformation and Temperature on Magnetic Characteristics of the Single-walled Chiral Toroidal Carbon Nanotubes. *Chinese Journal of Electronics*, 19(3), 423-426.

[69] Rodríguez-Manzo, J. A., López-Urías, F., Terrones, M., & Terrones, H. (2007). Anomalous Paramagnetism in Doped Carbon Nanostructures. *Small*, 3(1), 120-125.

[70] Castillo-Alvarado, F. d. L., Ortíz-López, J., Arellano, J. S., & Cruz-Torres, A. (2010). Hydrogen Storage on Beryllium-Coated Toroidal Carbon Nanostructure C_{120} Modeled with Density Functional Theory. *Advances in Science and Technology*, 72, 188-195.

[71] Hilder, T. A., & Hill, J. M. (2007). Orbiting atoms and C_{60} fullerenes inside carbon nanotori. *Journal of Applied Physics*, 101(6), 64319 .

[72] Lusk, M. T., & Hamm, N. (2007). Ab initio study of toroidal carbon nanotubes with encapsulated atomic metal loops. *Physical Review B*, 76(12), 125422.

[73] Mukherjee, B., Maiti, P. K., Dasgupta, C., & Sood, A. K. (2010). Single-File Diffusion of Water Inside Narrow Carbon Nanorings. *ACS Nano*, 4(2), 985-991.

[74] Koós, A. A., Ehlich, R., Horváth, Z. E., Osváth, Z., Gyulai, J., Nagy, J. B., & Biró, L. P. (2003). STM and AFM investigation of coiled carbon nanotubes produced by laser evaporation of fullerene. *Materials Science and Engineering: C*, 23(1-2), 275 -278.

[75] Saveliev, A. V., Merchan-Merchan, W., & Kennedy, L. A. (2003). Metal catalyzed synthesis of carbon nanostructures in an opposed flow methane oxygen flame. *Combustion and Flame*, 135(1-2), 27 -33.

[76] Bai, J. B., Hamon, A. L., Marraud, A., Jouffrey, B., & Zymla, V. (2002). Synthesis of SWNTs and MWNTs by a molten salt (NaCl) method. *Chemical Physics Letters*, 365(1-2), 184 -188.

[77] Ajayaghosh, A., Vijayakumar, C., Varghese, R., & George, S. J. (2006). Cholesterol-Aided Supramolecular Control over Chromophore Packing: Twisted and Coiled Helices with Distinct Optical, Chiroptical, and Morphological Features. *Angewandte Chemie*, 118(3), 470-474.

[78] Yamamoto, T., Fukushima, T., Aida, T., & Shimizu, T. (2008). Self-Assembled Nanotubes and Nanocoils from ss-Conjugated Building Blocks. *Advances in Polymer Science*, 220, 1-27.

[79] Lujun, P., Hayashida, T., Mei, Z., & Nakayama, Y. (2001). Field emission properties of carbon tubule nanocoils. *Japanese Journal of Applied Physics*, 40(3B), L235-L237.

[80] Jining, X., Mukhopadyay, K., Yadev, J., & Varadan, V. K. (2003). Catalytic chemical vapor deposition synthesis and electron microscopy observation of coiled carbon nanotubes. *Smart Materials and Structures*, 12(5), 744-748.

[81] Hou, H., Jun, Z., Weller, F., & Greiner, A. (2003). Large-Scale Synthesis and Characterization of Helically Coiled Carbon Nanotubes by Use of $Fe(CO)_5$ as Floating Catalyst Precursor. *Chemistry of Materials*, 15(16), 3170-3175.

[82] Zhong, D. Y., Liu, S., & Wang, E. G. (2003). Patterned growth of coiled carbon nanotubes by a template-assisted technique. *Applied Physics Letters*, 83(21), 4423-4425.

[83] Tang, N., Wen, J., Zhang, Y., Liu, F., Lin, K., & Du, Y. (2010). Helical Carbon Nanotubes: Catalytic Particle Size-Dependent Growth and Magnetic Properties. *ACS Nano*, 4(1), 241-250.

[84] Lau, K. T., Lu, M., & Hui, D. (2006). Coiled carbon nanotubes: Synthesis and their potential applications in advanced composite structures. *Composites Part B: Engineering*, 37(6), 437-448.

[85] Fejes, D., & Hernádi, K. (2010). A Review of the Properties and CVD Synthesis of Coiled Carbon Nanotubes. *Materials*, 3(4), 2618-2642.

[86] Shaikjee, A., & Coville, N.J. (2012). The synthesis, properties and uses of carbon materials with helical morphology. *Journal of Advanced Research*, 3(3), 195-223.

[87] Fonseca, A., Hernadi, K., Nagy, J. B., Lambin, P., & Lucas, A. A. (1996). Growth mechanism of coiled carbon nanotubes. *Synthetic Metals*, 77(1-3), 235 -242.

[88] Pan, L. J., Zhang, M., & Nakayama, Y. (2002). Growth mechanism of carbon nanocoils. *Journal of Applied Physics*, 91(12), 10058-10061.

[89] Chen, X., Yang, S., Takeuchi, K., Hashishin, T., Iwanaga, H., & Motojiima, S. (2003). Conformation and growth mechanism of the carbon nanocoils with twisting form in comparison with that of carbon microcoils. *Diamond and Related Materials*, 12(10-11), 1836-1840.

[90] Bandaru, P. R., Daraio, C., Yang, K., & Rao, A. M. (2007). A plausible mechanism for the evolution of helical forms in nanostructure growth. *Journal of Applied Physics*, 101(9), 094307.

[91] Dunlap, B. I. (1994). Relating carbon tubules. Physical Review B , 49(8), 5643-5651.

[92] Fonseca, A., Hernadi, K., Nagy, J. b., Lambin, P., & Lucas, A. A. (1995). Model structure of perfectly graphitizable coiled carbon nanotubes. *Carbon*, 33(12), 1759-1775.

[93] Ihara, S., Itoh, S., & Kitakami, J. i. (1993). Helically coiled cage forms of graphitic carbon. *Physical Review B*, 48(8), 5643-5647.

[94] Setton, R., & Setton, N. (1997). Carbon nanotubes: III. Toroidal structures and limits of a model for the construction of helical and S-shaped nanotubes. *Carbon*, 35(4), 497-505.

[95] Akagi, K., Tamura, R., Tsukada, M., Itoh, S., & Ihara, S. (1995). Electronic Structure of Helically Coiled Cage of Graphitic Carbon. *Physical Review Letters*, 74(12), 2307-2310.

[96] Akagi, K., Tamura, R., Tsukada, M., Itoh, S., & Ihara, S. (1996). Electronic structure of helically coiled carbon nanotubes: Relation between the phason lines and energy band features. *Physical Review B*, 53(4), 2114-2120.

[97] Biro, L. P., Mark, G. I., & Lambin, P. (2003). Regularly coiled carbon nanotubes. *Nanotechnology, IEEE Transactions on*, 2(4), 362-367.

[98] Liu, L., Gao, H., Zhao, J., & Lu, J. (2010). Superelasticity of Carbon Nanocoils from Atomistic Quantum Simulations. *Nanoscale Research Letters*, 5(3), 478-483.

[99] Zhong-can, O. Y., Su, Z. B., & Wang, C. L. (1997). Coil Formation in Multishell Carbon Nanotubes: Competition between Curvature Elasticity and Interlayer Adhesion. *Physical Review Letters*, 78(21), 4055-4058.

[100] Volodin, A., Ahlskog, M., Seynaeve, E., Van Haesendonck, C., Fonseca, A., & Nagy, J. B. (2000). Imaging the Elastic Properties of Coiled Carbon Nanotubes with Atomic Force Microscopy. *Physical Review Letters*, 84(15), 3342-3345.

[101] Hayashida, T., Pan, L., & Nakayama, Y. (2002). Mechanical and electrical properties of carbon tubule nanocoils. *Physica B: Condensed Matter*, 323(1-4), 352-353.

[102] Chen, X., Zhang, S., Dikin, D. A., Ding, W., Ruoff, R. S., Pan, L., & Nakayama, Y. (2003). Mechanics of a Carbon Nanocoil. *Nano Letters*, 3(9), 1299-1304.

[103] Huang, W. M. (2005). Mechanics of coiled nanotubes in uniaxial tension. *Materials Science and Engineering: A*, 408(1-2), 136 -140.

[104] Neng-Kai, C., & Shuo-Hung, C. (2008). Determining Mechanical Properties of Carbon Microcoils Using Lateral Force Microscopy. *IEEE Transactions on Nanotechnology*, 7(2), 197-201.

[105] Poggi, M. A., Boyles, J. S., Bottomley, L. A., Mc Farland, A. W., Colton, J. S., Nguyen, C. V., Stevens, R. M., & Lillehei, P. T. (2004). Measuring the Compression of a Carbon Nanospring. *Nano Letters*, 4(6), 1009-1016.

[106] Fonseca, A. F. d., & Galvão, D. S. (2004). Mechanical Properties of Nanosprings. *Physical Review Letters*, 92(17), 175502 .

[107] Fonseca, A. F. d., Malta, C. P., & Galvão, D. S. (2006). Mechanical properties of amorphous nanosprings. *Nanotechnology*, 17(22), 5620-5626.

[108] Coluci, V. R., Fonseca, A. F., Galvão, D. S., & Daraio, C. (2008). Entanglement and the Nonlinear Elastic Behavior of Forests of Coiled Carbon Nanotubes. *Physical Review Letters*, 100(8), 086807 .

[109] Ghaderi, S. H., & Hajiesmaili, E. (2010). Molecular structural mechanics applied to coiled carbon nanotubes. *Computational Materials Science*, 55(0), 344-349.

[110] Kaneto, K., Tsuruta, M., & Motojima, S. (1999). Electrical properties of carbon micro coils. *Synthetic Metals*, 103(1-3), 2578 -2579.

[111] Ebbesen, T. W., Lezec, H. J., Hiura, H., Bennett, J. W., Ghaemi, H. F., & Thio, T. (1996). Electrical conductivity of individual carbon nanotubes. *Nature*, 382(6586), 54-56.

[112] Chiu, H. S., Lin, P. I., Wu, H. C., Hsieh, W. H., Chen, C. D., & Chen, Y. T. (2009). Electron hopping conduction in highly disordered carbon coils. *Carbon*, 47(7), 1761-1769.

[113] Tang, N., Kuo, W., Jeng, C., Wang, L., Lin, K., & Du, Y. (2010). Coil-in-Coil Carbon Nanocoils: 11 Gram-Scale Synthesis, Single Nanocoil Electrical Properties, and Electrical Contact Improvement. *ACS Nano*, 4(2), 781-788.

[114] Fujii, M., Matsui, M., Motojima, S., & Hishikawa, Y. (2002). Magnetoresistance in carbon micro-coils obtained by chemical vapor deposition. *Thin Solid Films*, 409(1), 78-81.

[115] Liu, L., Gao, H., Zhao, J., & Lu, J. (2011). Quantum conductance of armchair carbon nanocoils: roles of geometry effects. *SCIENCE CHINA Physics, Mechanics & Astronomy*, 54(5), 841-845.

[116] Motojima, S., Chen, X., Yang, S., & Hasegawa, M. (2004). Properties and potential applications of carbon microcoils/nanocoils. *Diamond and Related Materials*, 13(11-12), 19895-1992.

[117] Volodin, A., Buntinx, D., Ahlskog, M., Fonseca, A., Nagy, J. B., & Van Haesendonck, C. (2004). Coiled Carbon Nanotubes as Self-Sensing Mechanical Resonators. *Nano Letters*, 4(9), 1775-1779.

[118] Bell, D. J., Sun, Y., Zhang, L., Dong, L. X., Nelson, B. J., & Grützmacher, D. (2006). Three-dimensional nanosprings for electromechanical sensors. *Sensors and Actuators A Physical*, 130-131(0), 54 -61.

[119] Kato, Y., Adachi, N., Okuda, T., Yoshida, T., Motojima, S., & Tsuda, T. (2003). Evaluation of induced electromotive force of a carbon micro coil. *Japanese Journal of Applied Physics*, 42(8), 5035-5037.

[120] Shaoming, Y., Xiuqin, C., Aoki, H., & Motojima, S. (2006). Tactile microsensor elements prepared from aligned superelastic carbon microcoils and polysilicone matrix. *Smart Materials and Structures*, 15(3), 687-694.

[121] Greenshields, M. W., Hummelgen, I. A., Mamo, M. A., Shaikjee, A., Mhlanga, S. D., van Otterlo, W. A., & Coville, N. J. (2011). Composites of Polyvinyl Alcohol and Carbon (Coils, Undoped and Nitrogen Doped Multiwalled Carbon Nanotubes) as Ethanol, Methanol and Toluene Vapor Sensors. *Journal of Nanoscience and Nanotechnology*, 11(11), 10211-10218.

[122] Lau, K. t., Lu, M., & Liao, K. (2006). Improved mechanical properties of coiled carbon nanotubes reinforced epoxy nanocomposites. *Composites Part A: Applied Science and Manufacturing*, 37(10), 18375-18405.

[123] Yoshimura, K., Nakano, K., Miyake, T., Hishikawa, Y., & Motojima, S. (2006). Effectiveness of carbon microcoils as a reinforcing material for a polymer matrix. *Carbon*, 44(13), 2833-2838.

[124] Li, X. F., Lau, K. T., & Yin, Y. S. (2008). Mechanical properties of epoxy-based composites using coiled carbon nanotubes. *Composites Science and Technology*, 68(14), 2876-2881.

[125] Sanada, K., Takada, Y., Yamamoto, S., & Shindo, Y. (2008). Analytical and Experimental Characterization of Stiffness and Damping in Carbon Nanocoil Reinforced Polymer Composites. *Journal of Solid Mechanics and Materials Engineering*, 2(12), 1517-1527.

[126] Katsuno, T., Chen, X., Yang, S., Motojima, S., Homma, M., Maeno, T., & Konyo, M. (2006). Observation and analysis of percolation behavior in carbon microcoils/silicone-rubber composite sheets. *Applied Physics Letters*, 88(23), 232115-232113.

[127] Yoshimura, K., Nakano, K., Miyake, T., Hishikawa, Y., Kuzuya, C., Katsuno, T., & Motojima, S. (2007). Effect of compressive and tensile strains on the electrical resistivity of carbon microcoil/silicone-rubber composites. *Carbon*, 45(10), 1997-2003.

[128] Nakamatsu, K., Igaki, J., Nagase, M., Ichihashi, T., & Matsui, S. (2006). Mechanical characteristics of tungsten-containing carbon nanosprings grown by FIB-CVD. *Microelectronic Engineering*, 83(4-9), 808 -810 .

[129] Bi, H., Kou, K. C., Ostrikov, K., Yan, L. K., & Wang, Z. C. (2009). Microstructure and electromagnetic characteristics of Ni nanoparticle film coated carbon microcoils. *Journal of Alloys and Compounds.*, 478(1-2), 796 -800 .

[130] Zhang, G. Y., Jiang, X., & Wang, E. G. (2004). Self-assembly of carbon nanohelices: Characteristics and field electron emission properties. *Applied Physics Letters*, 84(14), 2646-2648.

[131] Wu, X. L., Liu, Q., Guo, Y. G., & Song, W. G. (2009). Superior storage performance of carbon nanosprings as anode materials for lithium-ion batteries. *Electrochemistry Communications*, 11(7), 1468-1471.

[132] Raghubanshi, H., Hudson, M. S. L., & Srivastava, O. N. (2011). Synthesis of helical carbon nanofibres and its application in hydrogen desorption. *International Journal of Hydrogen Energy*, 36(7), 4482-4490.

[133] Motojima, S. (2008). Development of ceramic microcoils with 3D-herical/spiral structures. *Journal of the Ceramic Society of Japan*, 116(1357), 921-927.

[134] Motojima, S., Hoshiya, S., & Hishikawa, Y. (2003). Electromagnetic wave absorption properties of carbon microcoils/PMMA composite beads in W bands. *Carbon*, 41(13), 2658-2660.

IntechOpen